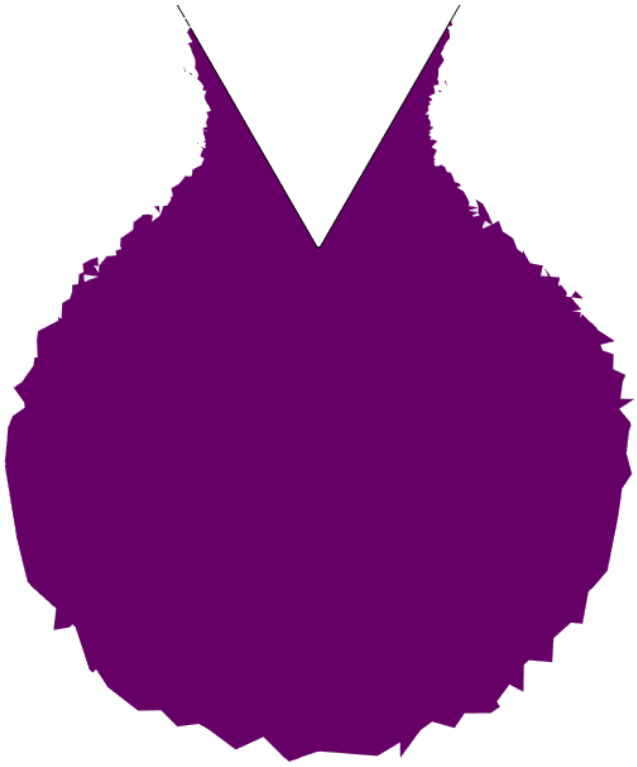

Water Tree Mapping in Submarine High Voltage Cables Using Finite Element Method

Master's thesis in Sustainable electric power engineering and electromobility

CARL-ADAM RYESKOG
HAZIM NOVLJANIN

DEPARTMENT OF ELECTRICAL ENGINEERING
CHALMERS UNIVERSITY OF TECHNOLOGY
Gothenburg, Sweden 2024
www.chalmers.se

Master's thesis 2024

Water Tree Mapping in Submarine High Voltage Cables Using Finite Element Method

CARL-ADAM RYESKOG
HAZIM NOVLJANIN

CHALMERS
UNIVERSITY OF TECHNOLOGY

Department of Electrical Engineering
Division of Electric Power Engineering
Chalmers University of Technology
Gothenburg, Sweden 2024

Water Tree Mapping in Submarine Power Cables Using Finite Element Method.
CARL-ADAM RYESKOG
HAZIM NOVLJANIN

Supervisor: Yuriy Serdyuk (Department of Electrical Engineering), Moon Moon Bordeori (Department of Electrical Engineering, Zhiyuan Li (Department of Marine Technology)
Examiner: Yuriy Serdyuk (Department of Electrical Engineering)

Master's Thesis 2024
Department of Electrical Engineering
Division of Electric Power Engineering
Chalmers University of Technology
SE-412 96 Gothenburg
Telephone +46 31 772 1000

Cover: Water tree pattern obtained from the simulation.

Typeset in LaTeX
Gothenburg, Sweden 2024

Water Tree Mapping in Submarine Power Cables Using Finite Element Method.
CARL-ADAM RYESKOG
HAZIM NOVLJANIN
Department of Electrical Engineering
Chalmers University of Technology

Abstract

Water treeing is a degradation phenomenon that occurs in submarine power cables. It is one of the main causes of failures of dynamic cables attached to mobile floating platforms. The rough sea environment causes mechanical stresses in the insulation of dynamic cables provoking appearance of microscopic cracks and water intrusion. The combination of water and enhanced electric fields can cause electrical, chemical, and mechanical reactions to occur which intensify water tree growth in cable insulation.

This thesis aims to contribute to the development of a numerical model for simulating water treeing in high voltage insulating materials. The scope of the thesis is limited to the electrical aspects of the water treeing. COMSOL Multiphysics is used to model the conditions for experimental water tree testing according to ASTM D6097 standard. The model considers the current flow in the polymeric insulation due to the applied electric stress and so-called state variable is used to map healthy and damaged regions in the insulation material. The latter is identified as a domain where the electric field exceeds the threshold corresponding to initiation of defects in the polymer due to appearing internal electrostatic forces. Validation is done by comparing the simulation to the standard and experiments reported in the literature. The results show that the numerical model follows previous observations and may be used as a base for further development of the tools for predicting insulation lifetime.

Keywords: water treeing, FEM, COMSOL, subsea cables, dynamic cables

Acknowledgements

First and foremost, we would like to express our gratitude to our supervisor and examiner Professor Yuriy Serdyuk. Your guidance, support, enthusiasm, and knowledge have helped and motivated us tremendously during this process.

Thank you to Postdoc Moon Moon Bordeori. Your kind words and willingness to help have been of great help to us. Good luck with your project. We wish you all the best for the future!

We would also like to express our thanks to Researcher Zhiyuan Li for his guidance during this process.

Lastly, to all of you who have brought ideas, been part of discussions, or in some way been a part of this journey - Thank you!

Carl-Adam Ryeskog & Hazim Novljanin, Gothenburg, June 2024

List of Acronyms

Below is the list of acronyms that have been used throughout this thesis listed in alphabetical order:

DEP	Dielectrophoresis
WT	Water tree
AC	Alternating current
DC	Direct current
PE	Polyethylene
XLPE	Cross-linked polyethylene
PMMA	Polymethyl methacrylate
PDE	Partial differential equation

Nomenclature

Below is the nomenclature of indices, sets, parameters, and variables that have been used throughout this thesis.

Parameters

t	Time
Δt	Time discretization step (time interval)
V	Voltage
timestep	Arbritrary time step

Variables

E	Electric field strength/ intensity/ stress (vector and magnitude)
D	Dielectric displacement density
J	Conduction current density
V	Voltage
I	Current
Q	Charge
R	Resistance
ϵ	Permittivity
σ	Conductivity

Contents

List of Figures

List of Tables

1

Introduction

1.1 Background

Today's society relies on steady supply of energy to meet its demands. Fossil fuels have been the main contributor to energy since the industrial revolution [5], but over the last decades, there has been a growing effort to replace fossil fuels with renewable energy sources to reduce the environmental impact. Solar, wind, and other renewable sources are more frequently used. In the case of wind power, the interest in off-shore wind power is increasing worldwide. One reason for this is that the wind speed off-shore is potentially higher than onshore, therefore higher energy production can be achieved [6].

The power generated at the off-shore power plants is delivered to the on-shore transmission substations through cables. Due to their location in the sea environment, such cables are exposed to specific conditions and, respectively, they should be desinged to meet specific requirements and secure reliable operation [7]. This is especially true for dynamic cables used for floating wind turbines and also for wave-energy converters. The rough environment causes stresses on the cable which can lead to water intrusion. Through the combination of water and localy enhanced electric fields, electrochemical reactions may take place which result in a insulation material degradation phenomenon called "water treeing". The growth of water trees can result in the appearance of relatively conductive regions within the insulation material which may provoke growth of so called "electrical trees" leading to insulation breakdown and failure [8]. Reparing failures of offshore installations come with a high cost, therefore proper maintenance of the cables is of high importance [6].

The service life of subsea cables is heavily dependent on the propagation of water trees within the cable and an understanding how the water tree develops within the cable insulation will aid in maintaining the cables, extending their lifetime and resulting in economic benefits. However, water treeing is mainly based on reported experimental observations and there is no commonly accepted numerical approach to simulate water treeing in power cables [3]. Therefore, in this work we have developed a numerical model to simulate the propagation of water trees in subsea cables and predict their properties.

1.2 Aim

This thesis project aims to contribute to the development of an interdisciplinary computational framework for simulations of water treeing in polymeric materials.

1.3 Scope and limitations

The focus is on electrostatic simulations to reveal electrical stresses acting on insulation material during tree growth. The theory chapter will cover general facts about water treeing to get a basic understanding of the phenomena. However, only the electrical aspect of the water tree propagation will be investigated in the simulation. The main focus lies on the feasibility of the model implementation. No experimental work is being done in the thesis and results obtained in the previous studies of water treeing will form the basis for verification of the model and underlying hypothesis. The model will implement experimental conditions as described in the international standard [2].

2

Phenomenology and characteristics of water trees in cable insulation

2.1 Water treeing

Water treeing is a phenomenon associated with initiation and growth of deterioration region in the insulation material of high voltage power cable. It is typically observed in polyethylene and cross-linked Polyethylene (XLPE) power cables. Water tress be described as localized zones of degradation, micro-channels, and microscopic chains of cavities [3]. A proposed definition describes that water tree degraded structures in polymers are permanent, grown due to humidity and electric field, having a lower electrical strength than the original polymer when wet, and are more hydrophilic than the original polymer [8].

This phenomenon is a major contributing factor to the decreased service life of power cables. Several factors contribute to the initiation, development and propagation of water trees including but not limited to defects, impurities, and micro-cavities as well as electrical and chemical properties. These properties and circumstances that marine power cables are subjected to also cause different types of water trees called bow-tie tress and vented tress. These will be described in more detailed in 2.1.1

As stated in the introduction, an absolute model that describes the water tree phenomenon has not yet been developed, but several models have been proposed based on electro-mechanical and chemical theory. This work will focus on the electrical theory.

2.1.1 Different types of water trees

Two major types of water trees have been identified, "bow-tie" and "vented" trees. These water tree types are named due to their respective characteristic geometrical pattern [1]. These two types of water trees are similar in many ways but have different features which affect their propagation and thereby the amount of damage done to the cable insulation.

2.1.1.1 Bow-tie trees

Bow-tie water trees are initiated inside the volume/bulk of the cables insulating material due to local impurities. The branches of this tree type propagate from the local initiation point radially along the electric field lines which gives it a "bow-tie" like shape. This water tree type is an uncommon cause of insulation breakdown since the maximum size that the water tree can grow into is limited by the amount of impurities contained in that local zone [1]. A typical bow-tie water tree can be seen in Figure 2.1.

Figure 2.1: Typical bow-tie tree in XLPE cable insulation [1].

2.1.1.2 Vented trees.

Vented water trees are initiated at the outer conductive screen of the cable at a localized point. This type of water tree propagates towards the inner conductive screen along the electric field through the insulating material. This means that with continuous access to water and other impurities, the vented tree can grow uninterruptedly through the insulation until the two electrodes are bridged [1]. A typical vented tree geometry can be seen in Figure 2.2.

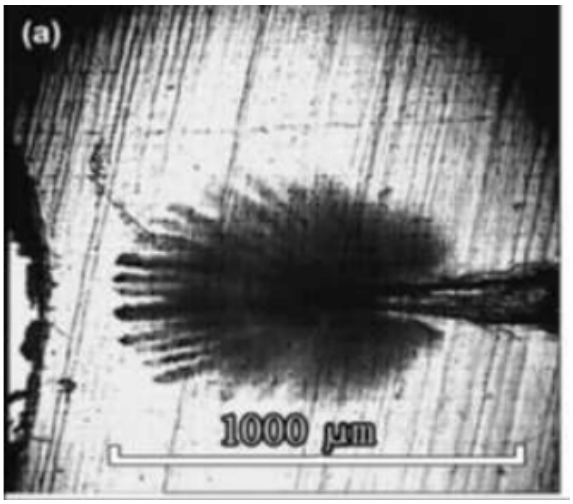

Figure 2.2: Typical vented tree in XLPE cable insulation [1].

Water tree growth for the "vented" tree is in the direction of the electrical field lines. Several branches grow and spread out from a localized point. Analysis of the tree structure using an optical microscope has proven that water trees are fractal objects and that their shape and structure have fractal tendencies [1]. Studies have shown that the electric field is more intensified at the regions closer to the conductor. Therefore, failures due to water treeing from vented trees initiated from the outer surface growing towards the conductor is more likely than other types of water trees [9]. In some cases, water trees may grow from the conductor side from the local field entrancement produced by defects on the inner semicon layer. This phenomenon is rather common for dynamic cables where moisture may diffuse along the conductor.

2.1.2 Electromechanical model of initiation and growth of water trees.

Water trees initiates and grown under certain conditions and are influenced by different mechanisms. It is a result of a synergy of electrical, mechanical and chemical processes. The reasons for water tree initiation are not fully understood and it is suggested that some physical phenomena may be more dominating than others [10].

Mechanical stress on a cable imposed by the oscillating forces of wave currents causes microscopic cracks in the cable insulation which are filled with water and other contaminants. As water diffuses into the insulating material, these water-filled microscopic defects with sharp edges locally enhance the electric field which in turn aids in the development of water trees [1][11]. A leakage current through the cable insulation containing such water filled microcavities causes accumulation of electric charges on polymer-water interfaces. Due to these interfacial charges, the insulation material is subjected to internal Maxwell forces which cause fractures and allows water tree branches to be initiated [11]. This may lead to additional charges at the interface between the polymer and the water which can additionally contribute to an enhancement of the electrostatic stress to the damaged area. Internal stresses within the dielectric material during the manufacturing processes may

also affects the water tree initiation. [8]. As a result of this, the local yield strength of the material may be lower than anticipated which means that small forces may be enough to initiate water trees. The permittivity increases with time during the growth of the tree due to the increase of water content [12]. In addition to water trees growing in the direction of the electric field, it has been found that water trees also tend to grow into regions where mechanical strains have been observed [8].

The growth rate of water trees is affected by the electrical stresses, in particular the magnitude and frequency of the applied voltage (electric field strength). Thus, it has been experimentally shown that frequency within the range of [30 - 445] kHz has a more significant impact on the growth of water trees than the electric field [13]. However, above this frequency range, water tree propagation does not appear to be influenced.

2.1.2.1 Dielectrophoresis phenomena in cable insulation material

The electromechanical model suggests that water tree development can be described by the theory of crack propagation in the material. However, electron microscopy experiments have shown that there are no cracks in the insulation where water trees are developed [8]. An alternative approach is to consider dielectrophoresis as a driving phenomenon of water treeing.

Dielectrophoresis (DEP) is related to the behavior of dielectric particles in inhomogeneous electric fields. A dipole with a zero net charge will experience polarization in an inhomogeneous electric field and respective force described by 2.1 where $\mathbf{p}$ is the induced dipole moment, $\epsilon_{1,2}$ are the permittivity of the particle and the surrounding dielectric medium respectively.

$$\mathbf{f} = (\mathbf{p} \cdot \nabla)\mathbf{E} = 2\pi\Re\frac{\epsilon_2(\epsilon_1 - \epsilon_2)}{\epsilon_1 + 2\epsilon_2}\nabla\mathbf{E}^2 \tag{2.1}$$

Depending on the relative permittivity of the dielectric medium and the particle, the particle will experience a force either in the direction or the opposite direction of the electric field gradient [14]. It has been observed that due to DEP, water molecules tend to move toward areas where the local field concentration is high [8].

Since water trees are grown in the presence of moisture and electric fields, DEP can be employed to provide a physical explanation of the mechanism of water tree growth. Since microscopic cracks on the cable sheath create localized strong and inhomogeneous electric fields, and also allow water to ingress, dielectrophoresis can explain how water particles are forced to diffuse into the insulating material and thereby create water trees.

2.2 Experimental investigations of water tree growth

Water trees are impossible to analyze when they grow into the insulating material of operational dynamic sub-sea cables, but they can be experimentally grown in a controlled lab environment. This allows for monitoring their electrical parameters and changes in the insulation due to water tree propagation. This also enables test samples to be exposed to the same conditions which aids in a fair comparison of water trees grown in different materials.

2.2.1 Water electrode method

Water tree growth is a slow process and the propagation and growth of a WT may take months or even years [9]. To accelerate the process, water electrodes in the form of a needle or a conical structure are often utilized. The conical needle acts as a defect in the insulating material creating a sharp geometrical shape in the test specimen which in turn creates an enhanced electric field around the tip.

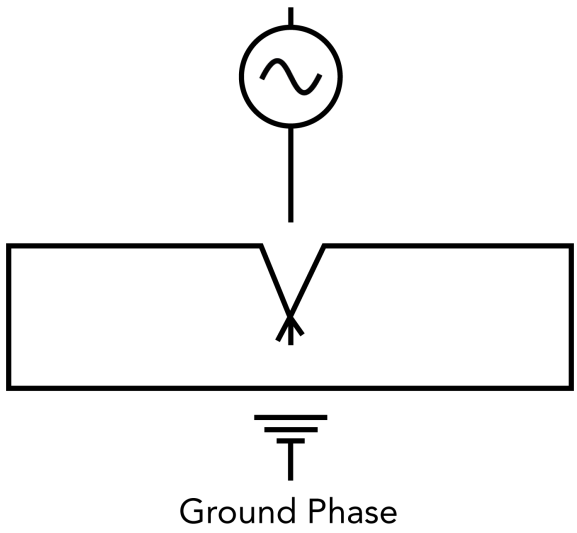

Figure 2.3: Sketch over a typical setup for the water electrode method.

The geometry of the material sample shown in Figure 2.7 often consist of a supporting plate, a insulation sample and a defect. Experimental conditions described in [2] are implemented in the numerical model developed in this thesis.

Figure 2.4: Typical shaped vented water tree according to the international standard ASTM D6097 [2].

2.2.2 Formation of void/air at the needle tip

It has been observed from previous studies that the thinner the diameter of the needle and the smaller point radius and point angle of the needle top, the more difficult it may be for the water electrode to be filled with water, which may result in the formation of an air layer in the tip of the needle, see figure 2.5.

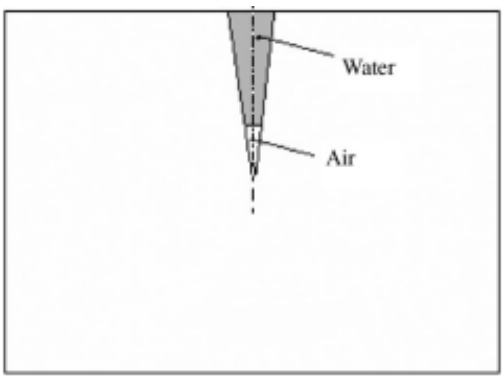

Figure 2.5: Double layer with an air layer at the tip of the water electrode [3].

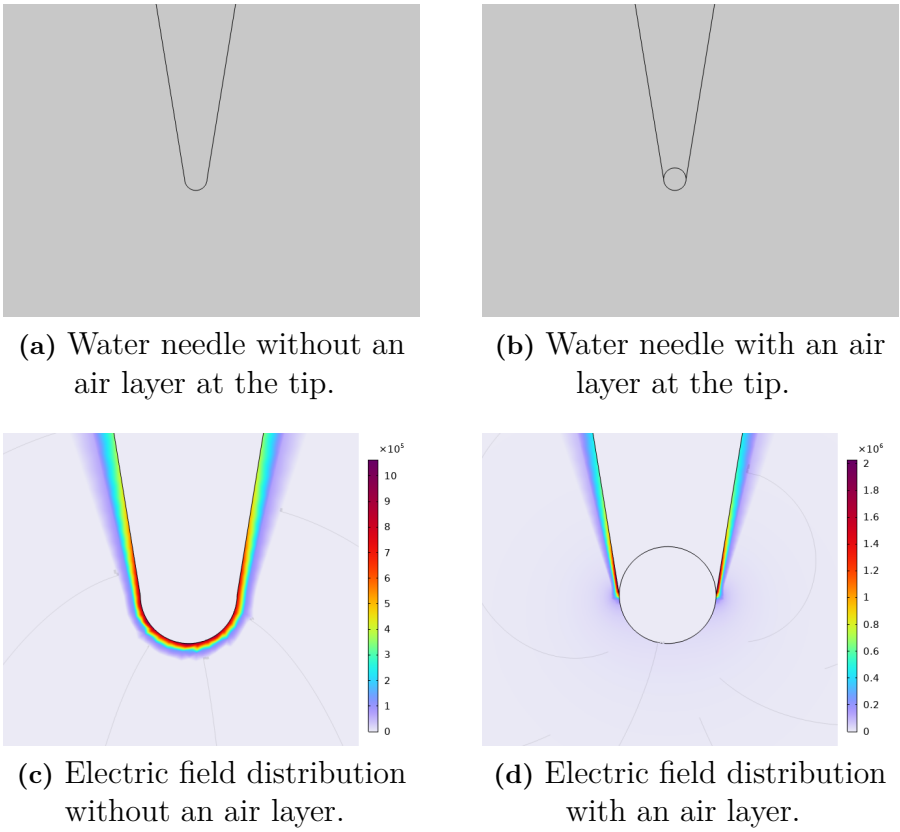

(a) Water needle without an air layer at the tip.

(b) Water needle with an air layer at the tip.

(c) Electric field distribution without an air layer.

(d) Electric field distribution with an air layer.

Figure 2.6: Comparison of the electric field distribution with and without the presence of an air layer.

This air layer influences local electric field distribution and may cause changes in the location of the highest stress as seen in Figure 2.6. Normally, the electric field is strongest at the tip of the conical defect if it fully filled with water, but because of the air layer, it has been observed that the field enhancement takes place at the triple junction between the water and air layers at the sides of the needle. This field enhancement at the interface may cause the water tree to initiate and grow perpendicular to the external electric field. It is also noted that different dimensions of the needle give different sizes of the propagated water tree [3].

2.2.3 Detection of water tree growth

A cross-section of a cable can be viewed as a capacitor with healthy insulation material between two electrodes where one electrode (central conductor) is connected to voltage supply and the other (external screen) to ground. The capacitance of the system can be determined according to equation 2.2.

$$C = \epsilon \frac{A}{d} \tag{2.2}$$

Evidently, the capacitance is a function of the dielectric constant ϵ multiplied by the geometrical factor accounting for the surface area of the electrode,A,divided by and the distance between them, d. While the dielectric constant does not change, the surface area and the distance are geometrical variables that may change due to the propagation of water trees. As the water tree grows into the healthy insulation medium in three dimensions, the distance between the electrodes becomes shorter while the surface area becomes larger which leads to an increase of the capacitance. Therefore, an indication of water tree growth is an increase in capacitance.

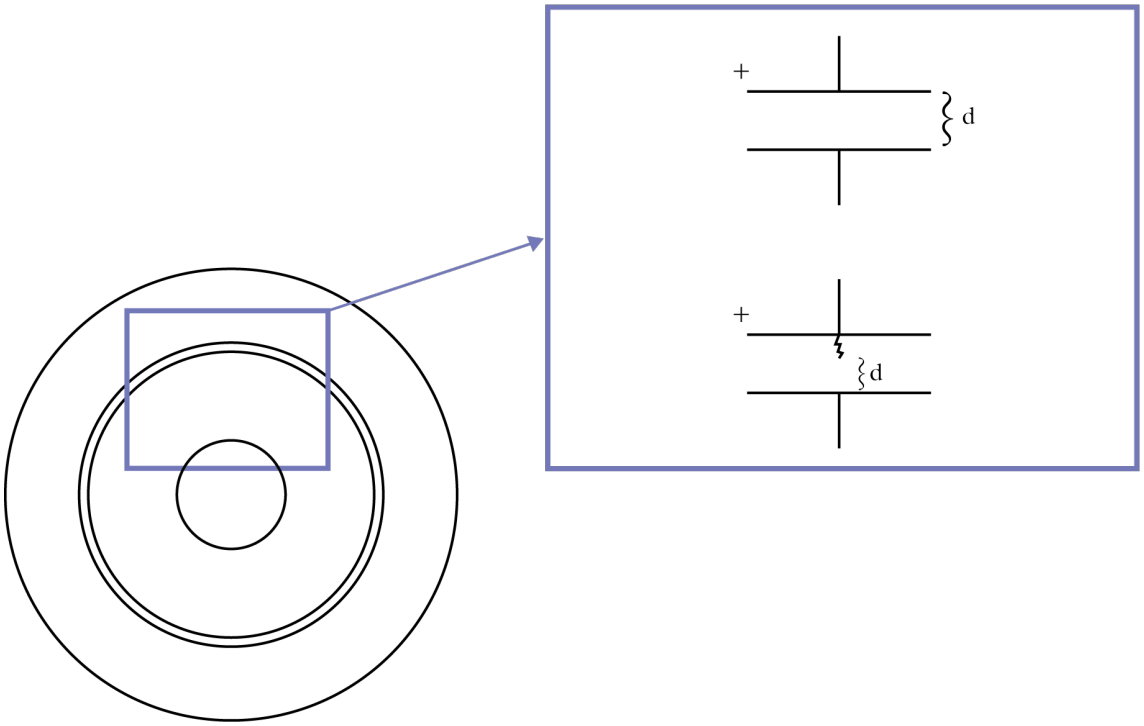

Figure 2.7: How a cross section of a cable can be interpreted as parallel plates.

There are several literature which explains about the increase in capacitance with increase in tree length. However, the results are not consistent [15][16][17][18]. The increase in capacitance based on previous research will be used as a reference point for the simulations done in this project. The experimental work used for comparison somewhat resembles the model created during this thesis and the water trees are grown to similar lengths.

Experimental water tree
Research have shown that the capacitance increases due to water tree propagation. By letting the water tree grow to $400\mu m$ the researchers found an increase from 12pF to 15pF which is an increase of 3pF [15].

Experimental electrical tree
Similarly, work on electrical detection of electrical trees in high voltage insulation materials have been conducted. Research shows that the increase in capacitance due to electrical treeing ranges around 20pF [16]. While electrical trees are not same as water trees, it is still interesting to see in what order of magnitude the measurements are being conducted.

Numerical water tree
Several researchers have attempted to determine the increase in capacitance through numerical simulations, these also vary depending on the model. Increase in capacitance may vary between 30pF - 70pF [17][18].

2.2.4 Parameters of water-treed region

Accelerated water tree aging experiments have established the groundwork suggesting how to model water-treed regions for numerical analysis. Since the degradation region of the insulation consists of water-filled microchannels and voids, it is not feasible to implement it directly due to extremely high space resolution required. For modeling purposes, it is usually assumed that properties of the damaged regions are different in permittivity and conductivity from those of the healthy material. In previous literature on numerical work, the parameters of the water treed region varies. The most common values used for various parts of the tree structure can be found in table 2.1 [19] [17].

Table 2.1: Water tree properties.

Water tree type	Conductivity [S/m]	Relative permittivity	Size [μm^2]	Shape
Water tree channel	10^{-17} - 10^{-7}	2.3 - 16	30	Rectangle
Water filled void/pore	$5.86 \cdot 10^{-6}$	80	15	Ellipse
Amorphous region	10^{-17} - 10^{-7}	2.3 - 10	-	-

In this thesis, a large amorphous region is investigated. The permittivity for such a region ranges from 2.3 to 10 while the conductivity ranges from 10^{-17} to 10^{7}S/m. While the permittivity is within a reasonable range, increasing from the initial value of 2.3, the value of the conductivity is not as suitable. The value of 10^{-17} [S/m] for a water-treed region indicates "healthier" properties than the value of 10^{-14} [S/m] for the main material. This means that when the water tree propagates into the insulation, the insulation gains better insulating properties. This is not reasonable and thereby only conductivity values ranging from 10^{-13} to 10^{-7} S/m will be modeled for the water-treed region.

2.3 Statistical model for non-ideal material properties

The propagation behavior of the water tree is dependent on the material properties of the dielectric medium. Usually, data from material manufacturers indicate just averaged values for e.g. electric conductivity or permittivity, which are adopted in computer models. Real materials, however, contain contaminants which may change the properties locally leading to local field enhancements. Localized stresses usually occurs inside the bulk of insulating material which is most likely to be a result of the manufacturing process. These localized regions of weakened material can be around the range of the yield strength of the material [8]. As mentioned earlier, WTs do not always propagate into regions where the electric field is the strongest but into regions where the yield strength of the material is lower [8].

The conductivity of a material is determined by applying a step voltage to a sample of the material and measuring the current through in time. Initially, capacitive effects are dominating and a polarization current is flowing through the material. When the relaxation of the polarization is achieved, the capacitive current vanishes and steady state is reached, the conductivity is determined from the steady state resistive current[20]. To analyze real material, one can imagine measuring the conductivity of a system, which is split into smaller parts as seen in figure 2.8, characterized by own local properties, $\sigma_m \neq \sigma_{x1,y1} \neq \sigma_{x2,y2}$.

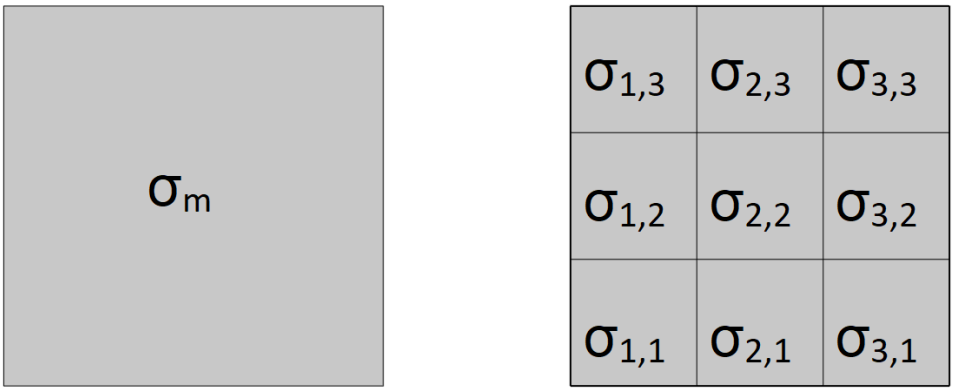

Figure 2.8: Conductivity of an entire system and individual parts of split up system.

Thereby, localized defects and weakened zones will be introduced into the dielectric to represent a realistic material. The proposed statistical models for realistic material modeling are based on normal distribution and Weibull distribution of the properties. Normal distribution parameters are easily calculated but is not suited for electrical data, while the Weibull distribution is the commonly accepted for solid insulation breakdown [21]. Therefore, the Weibull distribution is implemented in this study.

From the performed literature analysis, it is evident that the material properties of PE used for insulation of high voltage cables are not consistent in the existing literature, there are variations in recorded permittivity and conductivity found when conducting water tree testing Table 2.2 shows electrical parameters of PE from different manufacturers [4]. These values will not be used for this numerical model but they illustrate that there is a significant spread of properties reported by different materials manufacturers that makes it difficult to decide about specific values to use in the simulations.

Table 2.2: Variation of PE material properties from different manufacurers [4].

Material variant	Conductivity [S/m]	Dielectric constant
Polyethylene fibre (spectra 900)	$1.72 \cdot 10^{-19}$ - $1.72 \cdot 10^{-17}$	2 - 3
Chlorinated polyethylene (unreinforced)	$1.72 \cdot 10^{-19}$ - $1.72 \cdot 10^{-17}$	7 - 10
HDPE general purpose, molding, extrusion	$5.75 \cdot 10^{-25}$ - $5.22 \cdot 10^{-23}$	2.2 - 2.4
HDPE Low/medium molecular weight	$5.75 \cdot 10^{-25}$ - $5.22 \cdot 10^{-23}$	2.2 - 2.4
MDPE molding, extrusion	$1.72 \cdot 10^{-20}$ - $1.71 \cdot 10^{-19}$	2.3 - 2.5
LDPE (molding, extrusion)	$5.75 \cdot 10^{-24}$ - $5.22 \cdot 10^{-23}$	2.2 - 2.4
XLPE (molding)	$8.08 \cdot 10^{-23}$ - $7.22 \cdot 10^{-22}$	2.0 - 2.2

2.3.1 Phase state hysteresis transition

Hysteresis is a common phenomenon that can occur in a variety of physical systems. Generally, a hysteresis loop in a system can describe the behavior or state of said system depending of variations of depending factors [22]. In this thesis, a hysteresis loop function is used to describe the phase state and the transition of the phase state in the dielectric medium. This will simulate the development of water trees with respect to time since it is not a phenomenon that occurs instantly. Figure 2.9a shows an example of how a hysteresis loop can describe the state phase and change of phase state as a function of temperature and enthalpy. A material in a solid state will remain solid until the temperature reaches a sufficiently high value which forces a phase transformation. In order to transform back to a solid state again, the material has to drop to a lower temperature. The processes do not occur instantaneously, thereby the transition zones have a slight slope. This also aids in numerical computations.

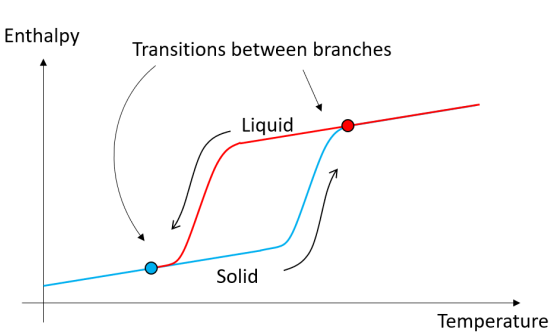

(a) Hysteresis loop illustrating change of phase state as a function of temperature[23].

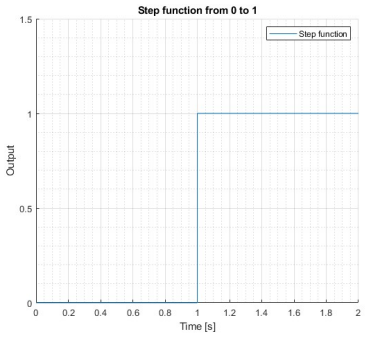

(b) Phase state based on a step function.

Figure 2.9: Phase state change functions.

For this thesis, a function described as a "transition function" which is based on a partial differential equation in coefficient form will be implemented in order to simulate the transition of a healthy material region to a water-treed region. Without a transition function it cannot distinguish between healthy and damaged region. A local region could attain both healthy and damaged status in a time sample which causes problems in the computations and the results. In Figure 2.9b, at time-step $1s$, a region can be interpreted as both healthy and damaged. This will cause computational errors and a solution that resembles the phase state transition in Figure 2.9a is needed.

3

The model and implementation

3.1 Modeling approach

The purpose of the model is to generate simulated water trees that are similar in shape to laboratory-grown water trees and that grow due to the same physical principles. Thereby a geometrical model is to be created that represents a real laboratory setup. The physics, parameters, and conditions are chosen to be close to real conditions. To realize this, the insulation material in which the water tree is grown is split up into what we refer to as healthy and damaged material regions which are simply a coordinate-based variation of material properties according to a statistical model which will be explained later. The philosophy behind this is based on the theory that water trees not only propagate into regions where the electric field is the strongest but also into regions where the material properties are weaker compared to surrounding regions. This means that the water propagation shape and rate are a function of the electric field stress applied to a region and the material characteristics and that specific region.

Furthermore, water trees are a phenomenon that may take several months or years in order to develop into a size that can be observed. To save time and computational power, the model is built around computing a series of discrete steady-state solutions where each solution is used as an initial condition for the next solution. This enables control of the propagation rate of the water trees. An analogy to this can be made, imagine starting to grow water trees in 10 identical laboratory setups. After a certain amount of time, one of the samples is taken out and examined, let us assume that there is a water tree present with a length of 100 μm. After the same amount of time, the next sample is examined which now has a water tree of 200 μm, and so on. This is the philosophy behind the discrete timesteps that are simulated in this project.

3.2 Model implementation

This section will describe how the computational model was created to reproduce conditions in the experimental setups used for accelerated water tree growth tests according to the international standard ASTM D6097-16, described in section 2.2.1.

3.2.1 Geometrical model

The geometrical model created in this thesis is built to mimic the setup recommended in the international standard ASTM D6097-16 [2]. This enables comparison between the numerical model and water-trees grown in a laboratory setup. Material used and their properties are described in section 3.2.2. The dimensions used in the numerical model can be found in Table 3.1.

Table 3.1: Dimensions for the geometry of the numerical model.

Quantity	Value [mm]
Insulation diameter	25.4
Insulation thickness	6.35
Defect diameter	4
Defect tip radius	0.003
Defect angle	60°
Defect depth	3.2
PMMA width long side	12.7
PMMA width short side	6.35
PMMA height	12.7

The test setup according to the international standard includes ten test specimens. In order to save computational power, the numerical model considers only one test specimen. The 3d gemoetry implemented in the model is shown in Figure 3.1 and a 2d slice of the geometrical model including materials assigned to each domain is shown in Figure 3.2.

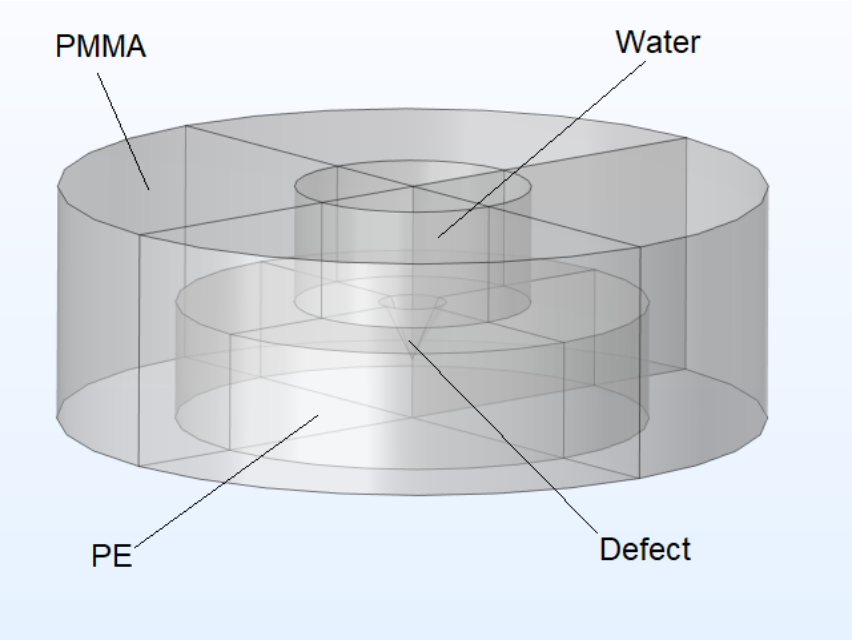

Figure 3.1: 3D geometry used in the thesis.

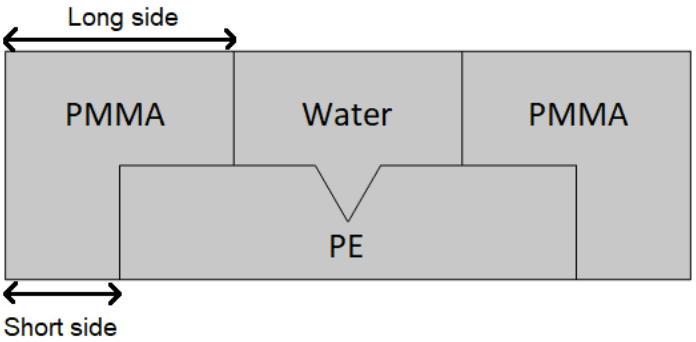

Figure 3.2: Geometrical model.

3.2.2 Material properties

The materials used are Polyethylene (PE) for the insulation sample, Poly(methyl methacrylate) (PMMA) for the supporting plate and saltwater as indicated in [2]. The amount of salt used in real testing is 292.2 ± 0.1 g solved in 5L deionized or distilled water at 20°C for 1.0 N NaCl, which gives a specific conductivity. This conductivity is used as the conductivity for the saltwater in the simulations. The material properties of the polyethylene test sample are taken from the material data sheet [24]. All properties are specified in table 3.2.

Table 3.2: Material properties.

Material	Conductivity [S/m]	Relative permittivity
Polyethylene	$1 \cdot 10^{-14}$	2.3
Saltwater solution	7.78	81
PMMA	$1 \cdot 10^{-15}$	3
WT region	10^{-13} - 10^{-7}	3.6 - 10

3.2.3 Physics and study

As described in sections 2.1.1 and 2.1.2, the phenomenon of water treeing can be explained by dielectrophoresis which describes how particles and charges move and behave due to forces acting upon them from inhomogeneous electric fields. Due to this, the Electric Currents (ec) interface is selected to compute electric fields, current, and potential distribution. This interface is used to solve the current continuity equation $\nabla J = 0$ which also takes into account the charges accumulated on materials interfaces. In the model, the current density, J, is the total current density including

both capacitive and resistive components. Since the propagation of water trees is a time-dependent phenomenon, it is essential to model it in the time domain. The following equations are solved in the Electric Currents (ec) interface for the time domain.

$$\nabla \cdot \mathbf{J} = Q_{j,v} \tag{3.1}$$

$$\mathbf{J} = \sigma \mathbf{E} + \frac{\partial \mathbf{D}}{\partial t} + \mathbf{J}_e \tag{3.2}$$

$$\mathbf{E} = -\nabla V \tag{3.3}$$

The current conservation domain solves the following equations:
Electric field, voltage gradient:

$$\mathbf{J}_c = \sigma \mathbf{E} \tag{3.4}$$

Dielectric displacement density, permittivity and electric field:

$$\mathbf{D} = \epsilon_0 \epsilon_r \mathbf{E} \tag{3.5}$$

The electric insulation domain solves the following equations:

$$\mathbf{n} \cdot \mathbf{J} = 0 \tag{3.6}$$

However, this is not feasible due to the extremely different time scales of the processes associated with treeing. Thus, charge transport through insulation takes place on a much shorter scale (minutes and hours) compared to the accumulation of material damages it causes that may take time from a couple of hundred days to several years. Therefore, in the present study the development of the water tree in the material is implemented as a sequence of steady states of the growing damaged region, D, in the healthy material, S. The expansion of the boundaries of this region is defined by the changes in the state variable which in turn are determined by the distribution of the electric field in the material domain. The repetition rate of the steady states in the modeled sequence is defined by the variable *timestep*, which is an auxiliary unit-less quantity having no relation to the actual time. For each new stationary solution that is to be computed, the previous solution is used as an initial condition. In this way, *timestep* can be viewed as a time step of an arbitrary value.

3.2.3.1 Boundary conditions, parameters and initial values

The domain and boundary conditions used in the model can be found in table 3.3. The purpose of the model is to replicate the test setup according to the international standard. Since *timestep* is defined as an arbitrary value, the voltage applied is defined as a ramp function that increases from 0 to 15V. This is due to the damage propagation being conditional upon the electric field stress. The propagation of the water tree damaged region is considered for at least 1500μm with steps of 100μm. The locations refer to the geometrical model described in Figure 3.2. The reason for the significantly lower voltage in this thesis compared to the international standard

is that it is a scaling factor. Lowering the voltage by a factor makes it possible to lower the water tree propagation condition and still arrive at the same results.

Table 3.3: Physics assigned to geometrical entities.

Description	Location	Selection	Value [V]
Current conservation	All domains	Domain	-
Electric insulation	Left, right & long side of PMMA	Boundary	-
Initial values	All domains	Domain	0
Ground	Bottom side of PE & short side PMMA	Boundary	0
Terminal	Water	Domain	Ramp function (0 - 15)

3.2.4 Implementing Weibull distribution

COMSOL multiphysics assigns material properties to each mesh element according to predefined values by the user. This results in materials assigned to a geometrical entity being represented as ideal which is not representative for a real case. Commonly, materials attain localized zones of weakness, impurities, and defects during the manufacturing process and during operation. This leads to in-homogeneous material structures properties of which can be represented by the Weibull distribution as described in section 2.2.

Local deviations of the material properties are implemented by a random distribution which can be obtained by an inbuilt COMSOL function 3.7

$$rn = 0.5 + random(x, y, z) \tag{3.7}$$

This function generates a uniformly distributed number between -0.5 and 0.5 to each set of (x,y,z) coordinates, the addition of 0.5 raises the boundaries to 0 and 1. By using this uniformly distributed random number as the argument for the inverse cumulative Weibull distribution function 3.8, and by varying the scale parameter (α) and shape parameter (β), it is possible to generate a spread of material properties.

$$we = \alpha \cdot \sqrt[\beta]{ln(\frac{1}{rn})} \tag{3.8}$$

There are no standard values for α and β to represent inhomogeneities in polyethylene, the values can vary significantly depending on manufacturing process and the way the material is treated before operation. In the present study, the scale parameter α is kept constant at a value of 1 while the shape parameter β varies between 2 and 100. Table 3.4 presents minumum, average and maximum values of we in the spatial domain.

Table 3.4: Weibull variables.

α	β	we_{Min}	we_{Avg}	we_{Max}
1	2	0.0019	0.8835	3.9466
1	50	0.7786	0.9887	1.0564
1	100	0.8824	0.9942	1.0278

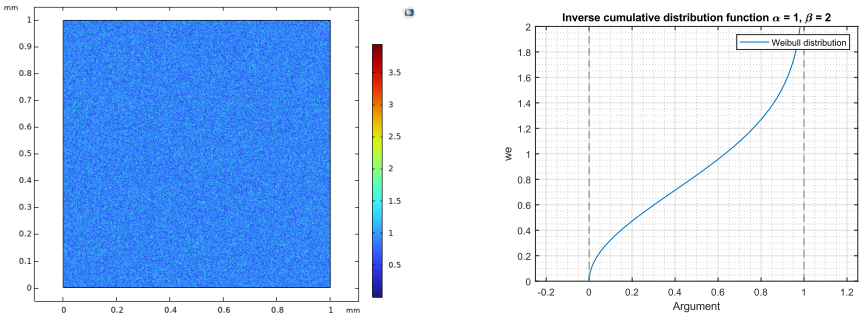

(a) $\beta = 2$.

(b) $\beta = 2$.

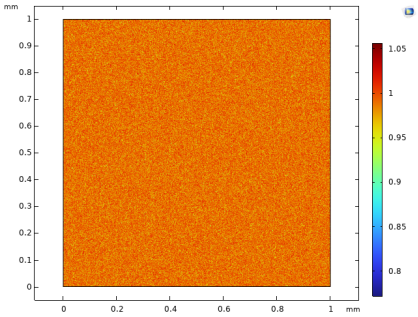

(c) $\beta = 50$.

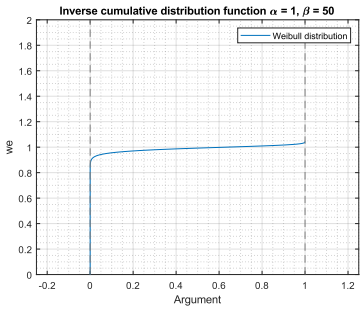

(d) $\beta = 50$.

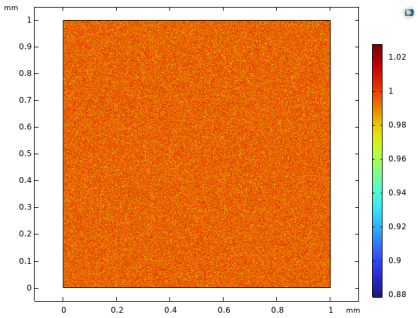

(e) $\beta = 100$.

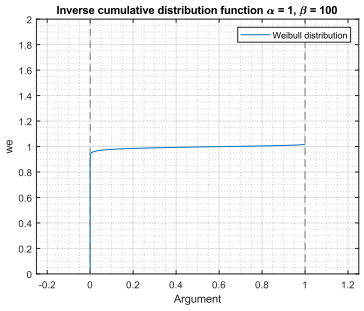

(f) $\beta = 100$.

Figure 3.3: Weibull distribution spatial plot in COMSOL and function plot.

The values assigned to the spatial coordinates from we is multiplied with the material properties to give the statistical spread according to 3.9 and 3.10.

$$\sigma_m = \sigma_{PE} \cdot we \tag{3.9}$$

$$\epsilon_m = \epsilon_{PE} \cdot we \tag{3.10}$$

The material inhomogeneties in the spatial domain is illustrated in Figure 3.3 a, c, e and g while the corresponding function plot can be found in Figure 3.3 b, d, f and h.

3.3 COMSOL multiphysics state variable

COMSOL Multiphysics state variable is a function that allows the user to track the history and changes of a model's domain, boundaries, edges, and points by implementing pre-defined conditions. The settings section in state variables allows the user to update the state variable before or after every parametric step. It is also possible to control how many points within an element are saved. By implementing conditions and coupling other functions with the state variable, it is possible to control physical properties in the geometrical entity that the state variable is applied to [23].

For this study, a state variable defined as "Damage" for the material volume occupied with the water tree is created and assigned as a sub-domain in the model. This state variable represents the initially solid and healthy insulation material, **S**, which is later transformed to the degraded material characterized by the properties of water treed polyethylene **D**. Thus, the state variable is defined according to 3.11 where **D**=damaged domain, and **S**=solid domain.

$$d(x,y,z) := \{d|d(x,y,z) \in [0,1], d(x,y,z) = 0 \forall d(x,y) \in \mathbf{S}, 0 < d(x,y,z) \leq 1 \forall d(x,y,z) \in \mathbf{D}\} \tag{3.11}$$

3.3.1 Implementation of state variable

The previously mentioned state variable "Damage" which is defined according to equation 3.11 has an initial value of 0 and it is updated expression according to equation 3.12, where $E\_breakdown = 10000$ [V/m]. This significantly lower value of the electric field is due to the applied voltage being lower compared to the value described in the international standard, it is possible to increase the applied voltage but one should also increase the propagations condition in order to arrive at the same results.

$$if(ec.normE > E\_breakdown, 1, Damage) \tag{3.12}$$

This expression states that if the electric field stress computed in a mesh element is larger than the predefined value of $E\_breakdown$, the state variable "Damage" attains a new value of 1 in the mesh node where the condition is fulfilled. In the remaining mesh nodes, "Damage" remains unchanged and equal to 0.

The state variable "Damage" is then used to affect the physics of the model to accurately represent the initiation and propagation of the water tree.

This state variable is linked to the conductivity σ_m and permittivity ϵ_m of the insulating material via a transition function which is described in section 3.3.2.

The objective of the state variable is to track local variatiions of the electric field in the insulating domain induced by the current flow and to monitor if a region is to be damaged due to the electric field stress or not.

3.3.2 Transition function

The state variables function sets an initial value of 0 to the variable "Damage" and is only changed to 1 if 3.12 is fulfilled, there are no values between 0 and 1 that can be set to "Damage". This causes problems in the computations since there is no transition period for the material to go from a healthy state to a damaged state. To solve this problem a transition function will be implemented.

A new interface called "Coeficcient form PDE (c)" was introduced and set to the insulation domain. This interface introduces 3.13 to the model which can be controlled by the the variables $e_a, d_a, c, \alpha, \gamma, \beta, a$, and f. In this case, u is the field variable, while f is the source term that is used to control how the PDE behaves.

$$e_a \frac{\partial^2 u}{\partial t} + d_a \frac{\partial u}{\partial t} - \nabla \cdot (c \cdot \nabla u + \alpha u - \gamma) + \beta \cdot \nabla u + au = f \tag{3.13}$$

The values chosen for the PDE variables can be found in 3.5.

Table 3.5: Variable values for PDE.

PDE variable	Value
e_a	0.001
d_a	0.1
c	f
α	0
γ	0
β	0
a	1
f	Damage

These values are choosen by trial and error in order to achieve a transition between 0 and 1 within a specific time. When the state variable "Damage" is 0, the source term is 0 and the transition function behaves according to 3.4a. When "Damage" is set to 1, the source term changes to 1 instantly and the transition function behaves according to 3.4b, increasing from 0 to 1 in a smooth way.

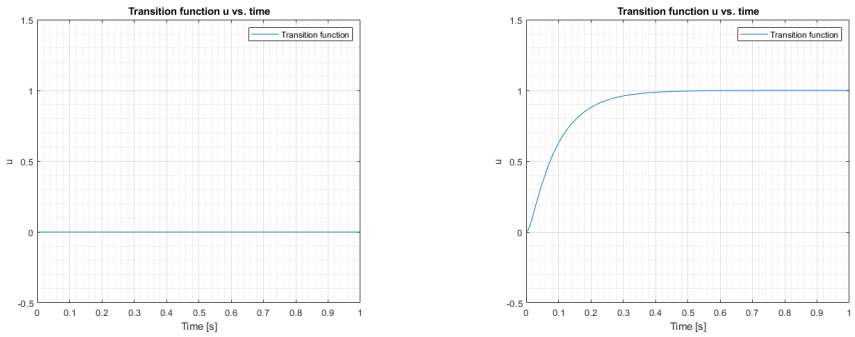

(a) Damage = 0. **(b)** Damage = 1.

Figure 3.4: Transition function behaviour for different values of Damage.

The field variable u is used to create a new state variable called $tran$ which has an initial value of 0 and is updated using the expression of u. This new state variable is used to update the conductivity and permittivity of the damaged regions in the insulating material according to 3.14 and 3.15. The values for σ_w and ϵ_w are explained in section 2.2.4.

$$\sigma_m = \sigma_{PE} \cdot we + tran \cdot \sigma_w \tag{3.14}$$

$$\epsilon_m = \epsilon_{PE} \cdot we + tran \cdot \epsilon_w \tag{3.15}$$

3.3.3 Mesh

The mesh statistics is in table 3.6 while an overview of the mesh can be seen in figure 3.5. To save computational time, the three materials used had different mesh settings since all areas were not equally interesting. A refine function is used inside the PE region around the needle tip where the tree is supposed to propagate to ensure a good result. Mesh is an important factor in the simulation and to make sure that the trade-off between computational time and mesh quality was in an acceptable range, the trial and error approach was utilized. When the result didn't change with a denser mesh, a courser mesh providing the same result was used for the simulation.

Table 3.6: Mesh statistics.

Material	Number of elements	Maximum element size	Minimum element size	Average element quality
PE	2 571 135	0.762 mm	0.00762 mm	0.648
PMMA	6075	3.05 mm	0.381 mm	0.6689
Water	506 954	3.05 mm	0.381 mm	0.6542

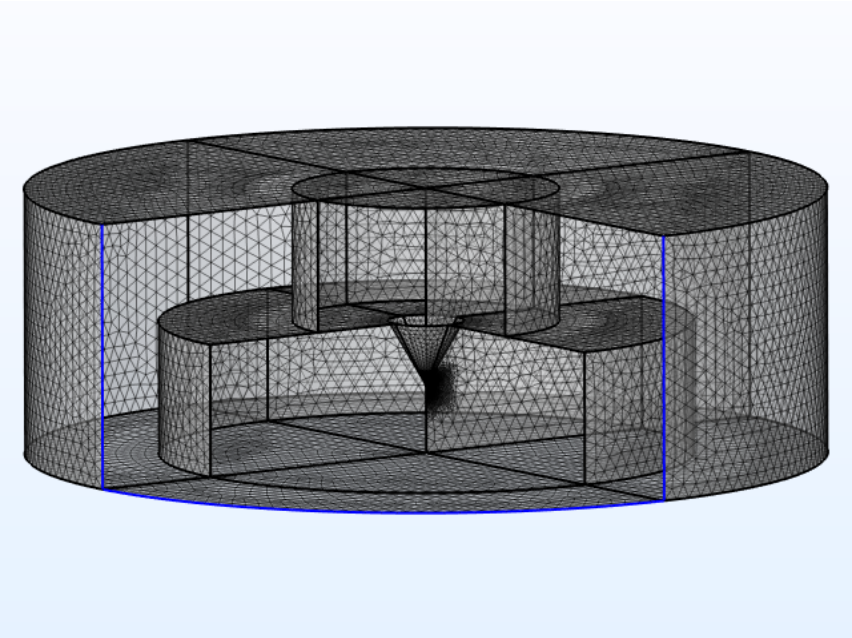

Figure 3.5: Overview of the mesh over the model.

4

Results of the simulations and discussion

4.1 Sensitivity analysis of water tree properties

This section presents how the capacitance varies due to the increase in length of the water tree as well as the propagation behavior of the water tree into the healthy insulating material. As per the literature, the material properties vary in the damaged region. Therefore, a parametric sweep is done with varying combinations of conductivity and permittivity. For each combination of these parameters, capacitance with respect to tree length is documented as well as propagation behavior. The conductivity is swept from 10^{-13} to 10^{-7}, and the permittivity from 3.6 to 10 for the water-treed region.

A typical water tree with its characteristic shape, size, and defined regions can be seen in Figure 4.1. This is used for illustrative purposes in order to continue with the results. It is important to note that in this thesis, water tree size can refer to two different things which are water tree length and volume. The water tree length is defined as the length of the tree starting from the needle tip to the opposite electrode, while the volume of the tree is the total volume in which we have a water tree. A water tree can be long and narrow which results in a tree with a significant tree length but small volume, on the other hand it can also be short and broad which means that the tree is shorter in length but larger in volume compared to the water tree described prior to this one.

Due to the difficulty of presenting three dimensional water trees in figures, the results will only illustrate two-dimensional slices of the insulating domain, however, the volume of each respective tree will be compared in graphs.

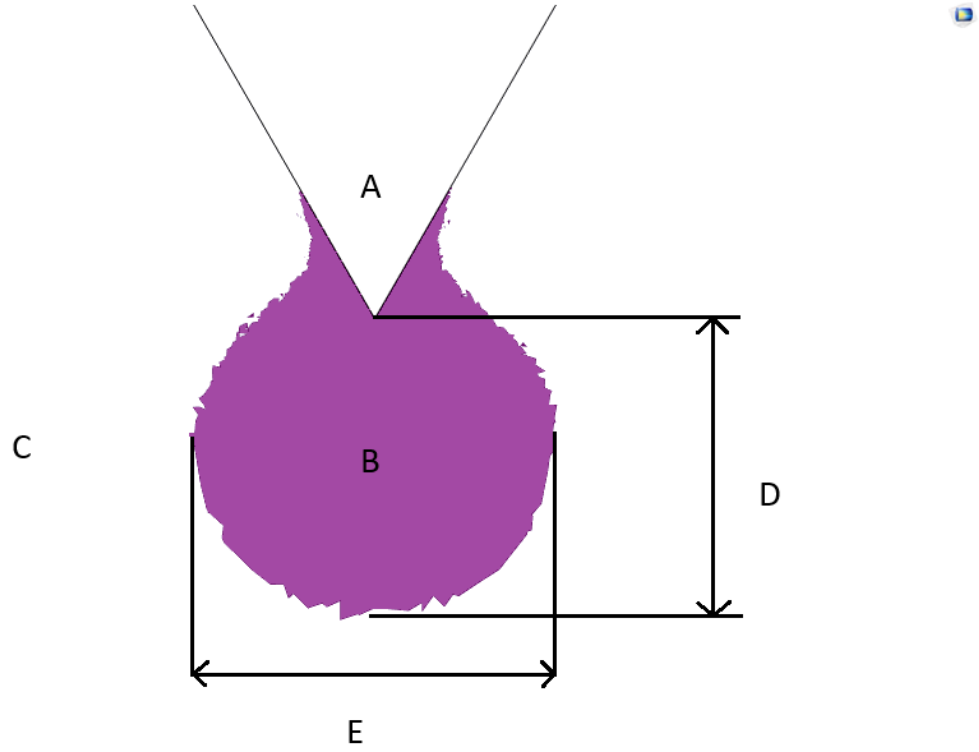

Figure 4.1: Typical shaped vented water tree where A: water needle electrode, B: water treed region, C: healthy insulating material, D: water tree length, and E: water tree width.

The water trees simulated in this thesis are grown from 0 μm to approximately 1500 μm. While the water tree lengths are roughly the same during each timestep and propagate with a length of approximately 100 μm for each timestep, it should be noted that the lengths are not exact for each water tree and can thereby not be used as a comparing factor. The volumes of the different water trees have been computed and will be used as a reference point when comparing the water trees. Therefore, the volume of the water tree will serve as a size comparison for the different trees when varying the conductivity and the permittivity of the water treed region while the length will serve in comparing the propagation rate in order to see at which timestep the water trees have grown to approximately 1500 μm.

The propagation behavior of the water trees can be seen in Figure 4.2 as the water tree grows from 0 to 400 μm. For varying conductivity and permittivity, no visible differences are observed during the first 400 μm.

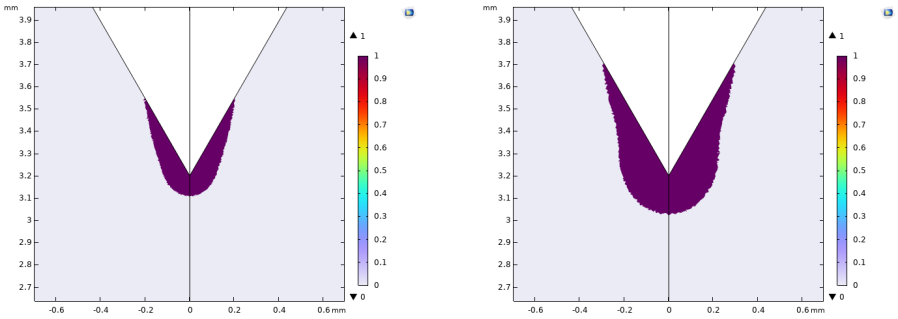

(a) $100\mu m$.

(b) $200\mu m$.

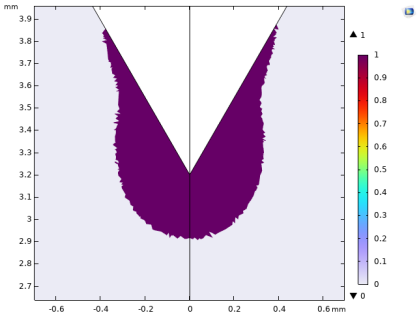

(c) $300\mu m$.

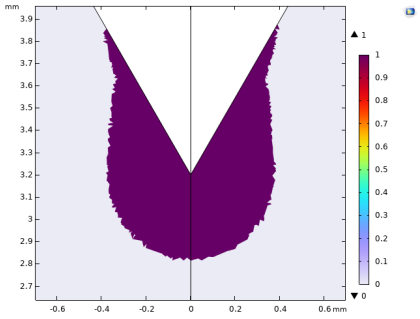

(d) $400\mu m$.

Figure 4.2: WT propagation behaviour and length from 0 to $400\mu m$.

However, when the water tree reaches lengths close to 1500 μm, there are significant differences in the shape. Figure 4.3a shows the water tree shape when the conductivity is set to 10^{-13} S/m while Figure 4.3b shows the shape when the conductivity is set to 10^{-7} S/m. Different values of permittivity do not affect the water tree shape significantly.

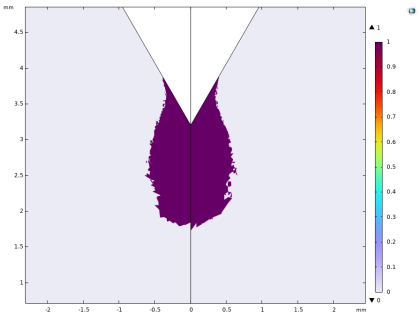

(a) Low conductivity.

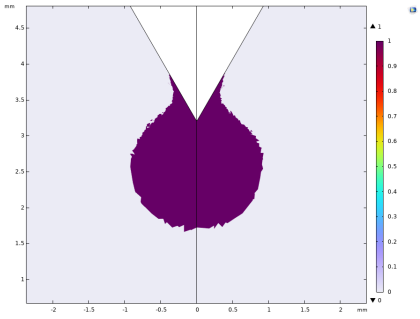

(b) High conductivity.

Figure 4.3: WT propagation behavior at a length of $1500\mu m$.

Figure 4.4 shows how the electric field first is strongest at the tip of the needle, but as the water tree grows and the damaged area increases, the strongest electric field strength is at the boundary between the healthy and the damaged region. Due to the different material properties, the electric field follows the water tree propagation which further increases the damaged region.

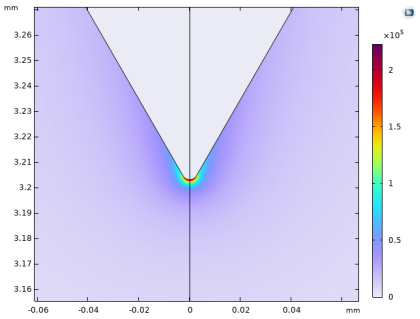

(a) Electric field with absence of water tree.

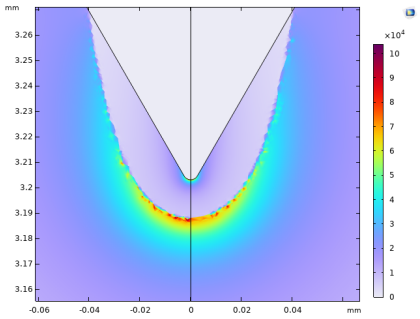

(b) Electric field with a small water tree.

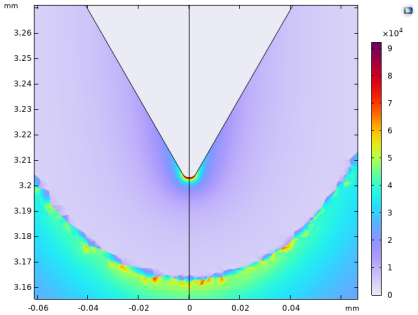

(c) Electric field with a larger water tree.

Figure 4.4: Electric field propagation.

Figure 4.5 shows how higher values for the conductivity result in larger water trees by volume for the same tree lengths. For shorter water tree lengths the volume appears to be smaller for larger values of conductivity. Looking at the water tree length of 1500 μm, water trees with higher conductivity are nearly twice as large compared to the ones with lower conductivity.

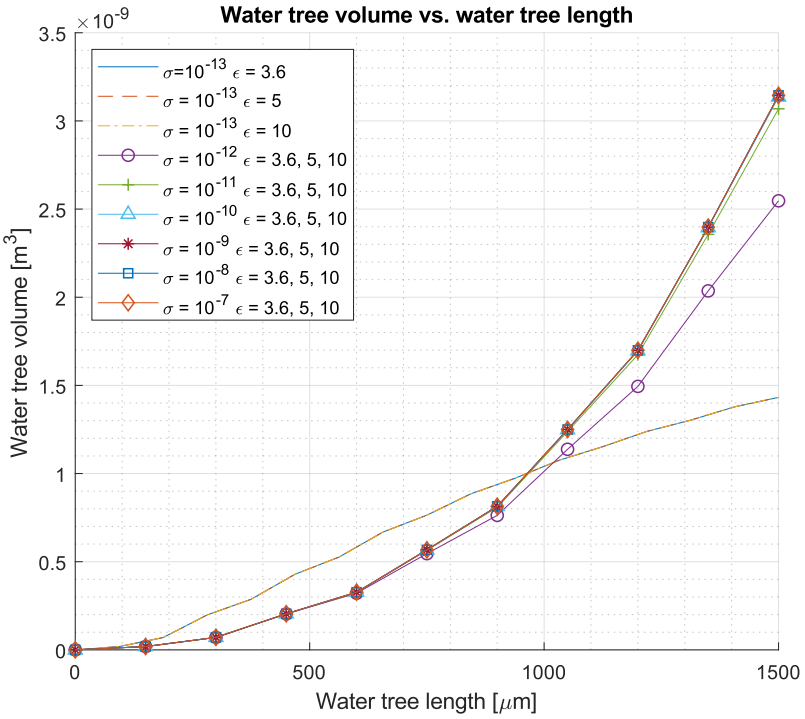

Figure 4.5: Water tree volume vs. water tree length.

Interesting to see is the propagation rate of the water trees, figure 4.6 shows the timesteps at which the water trees have developed to a specific size. It can be noticed that a higher conductivity, the water tree propagates faster compared to low conductivity value. For higher values of conductivity, the water tree reaches the full tree length of $1500\mu m$ in nearly half the timesteps compared to lower values of conductivity.

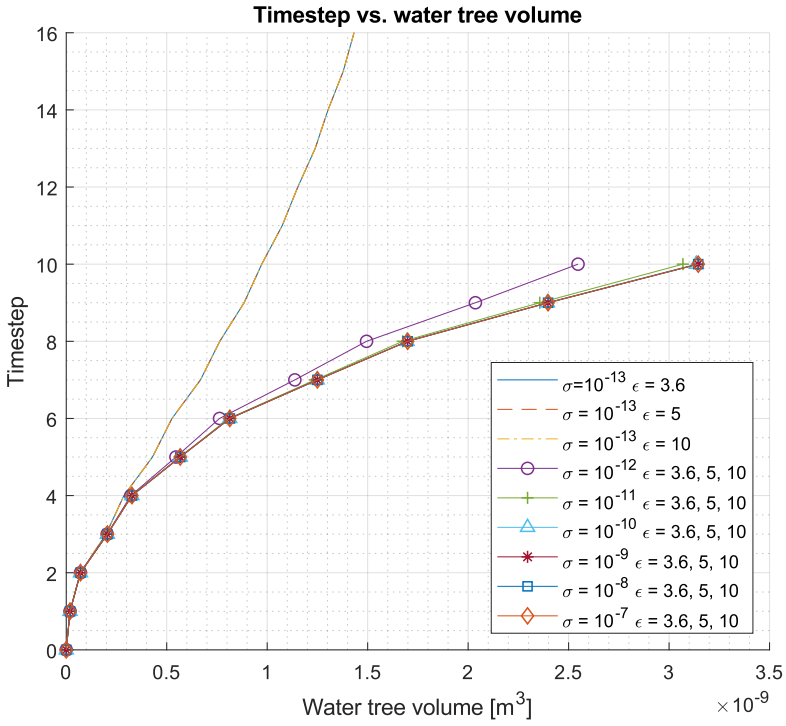

Figure 4.6: Times vs. water tree length.

The initial capacitance of the system without any water trees was computed to $1.9671pF$. Figure 4.3 shows the variation of capacitance with respect to the water tree volume for different conductivity and permittivity values of the water-treed region. For the lowest value of conductivity 10^{-13} S/m, an increase in permittivity will lead to an increase in capacitance. However, as the conductivity increases, the effect of permittivity with respect to the capacitance becomes negligible

It is seen that the capacitance increases as the conductivity increases. The higher values of conductivity results in larger water tree volume.

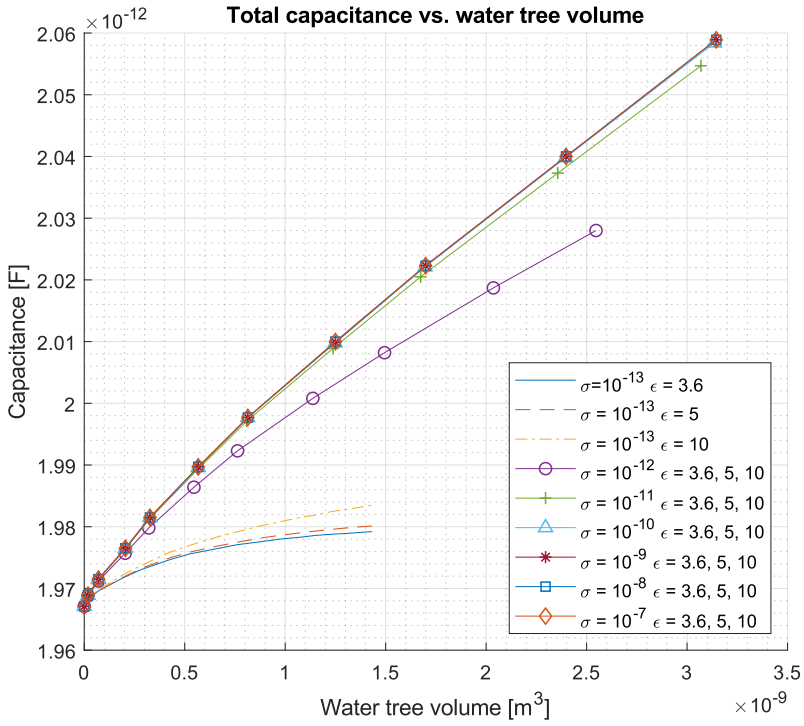

Figure 4.7: Total capacitance vs. water tree volume.

Figure 4.8 illustrates the increase in capacitance with respect to the water tree volume. Depending on the values of permittivity and conductivity, capacitance changes from $0.0121 - 0.910$ pF.

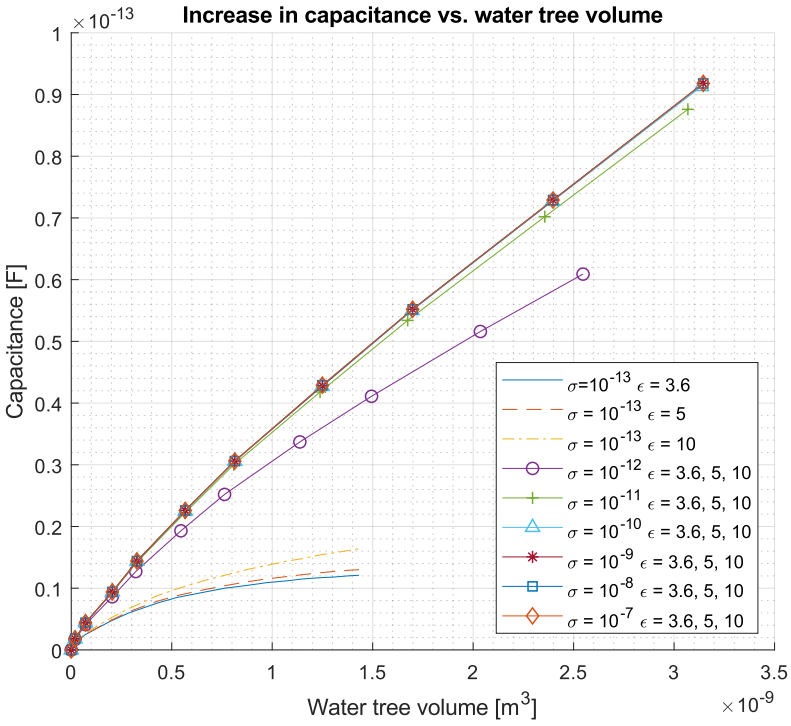

Figure 4.8: Total capacitance vs. water tree volume.

4.2 Air layer at water needle electrode tip

This section presents the influence of an air layer at the needle tip. According to the theory, there may be circumstances that create an air layer while conducting the water tree experiment. As described in the theory it has been theorized that the presence of the air layer at the needle tip will counteract the propagation of the water tree. The simulations are conducted with the same conditions and the images shown in Figure 4.9 are at the same time step. The only difference is the presence of an air layer indicated by the line in both figures. In Figure 4.9a the water treeing is propagating as expected by the tip of the needle, but in Figure 4.9b there is no propagation at the tip but instead at the interface between the two mediums.

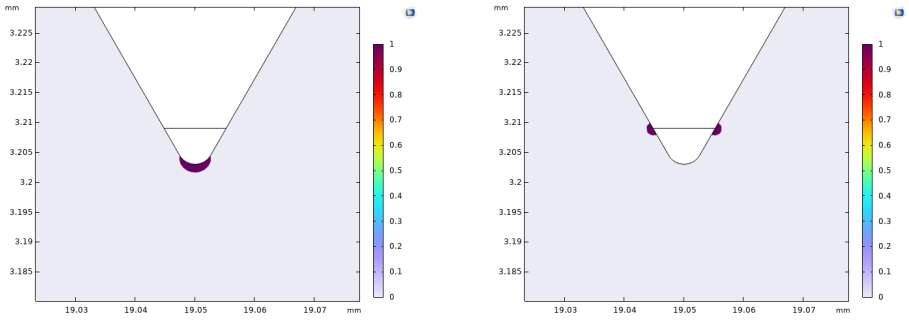

(a) No air layer present. **(b)** Air layer present.

Figure 4.9: Impact of an air layer in the water electrode.

4.3 Effect of material inhomogeneities

Regarding the effects of material inhomogeneities, the two extreme cases from the parametric sensitivity analysis, $\sigma = 10^{-7}$S/m and $\sigma = 10^{-13}$S/m, were selected to undergo further investigation. As stated earlier alpha is kept as 1, while beta is set to either 2, 50, or 100. This means that the material properties are multiplied by the value alpha which in turn has a statistical variance that is dependent on beta. These material inhomogeneities can be regarded as local weakend zones or pores with impurities. Introducing material inhomogeneities did not have a significant impact on the overall shape of the water tree. However, in addition to the vented tree, something resembling bow-tie trees were created close to the water electrode and the water tree. These bow-tie trees are seen as small outlying dots in Figure 4.10a and 4.10b.

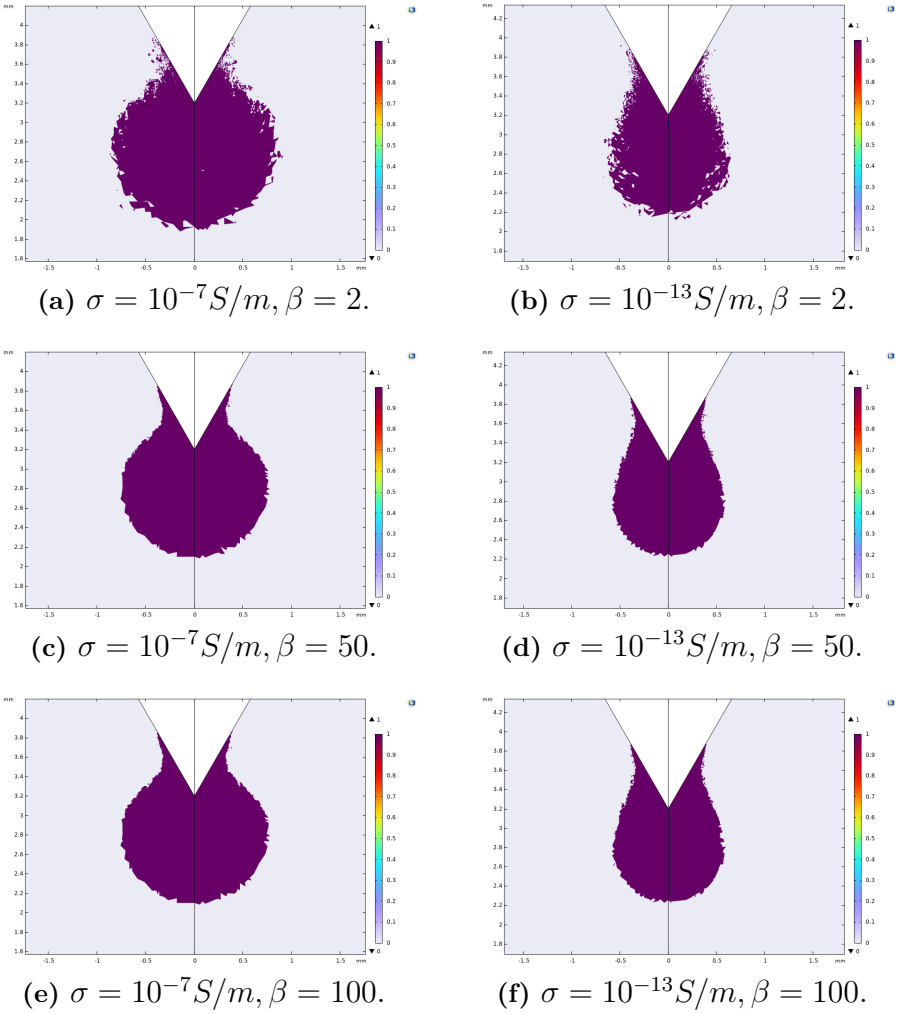

(a) $\sigma = 10^{-7}S/m, \beta = 2.$ **(b)** $\sigma = 10^{-13}S/m, \beta = 2.$

(c) $\sigma = 10^{-7}S/m, \beta = 50.$ **(d)** $\sigma = 10^{-13}S/m, \beta = 50.$

(e) $\sigma = 10^{-7}S/m, \beta = 100.$ **(f)** $\sigma = 10^{-13}S/m, \beta = 100.$

Figure 4.10: Water tree shape for the two extreme cases of $\sigma = 10^{-13}S/m$ and $\sigma = 10^{-13}S/m$ for different values of β.

When looking at the impact of the capacitance seen in figure 4.11, the shape parameter of $\beta = 2$ has a significant impact on the overall capacitance of the system. The total capacitance was decreased by approximately 0.1pF for conductivity values of 10^{-13} and 10^{-7} S/m. For the water tree with a conductivity of 10^{-13} S/m, it can be observed that the total volume of the water tree has increased but there is a slight decrease in capacitance compared to the results found in Figure 4.7. This is due to the weakened material properties is a result from the weibull distribution. The distribution affects the initial material properties and and properties of the water-treed region.

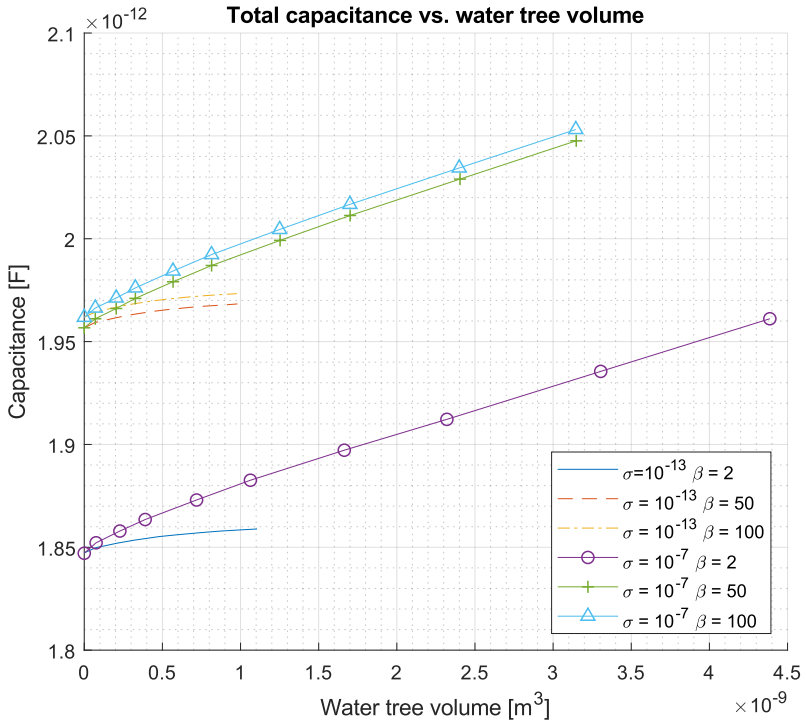

Figure 4.11: Total capacitance vs. water tree volume.

5

Conclusion

5.1 Conclusions from the results

This thesis has implemented a previously untested method for simulating water tree growth which i based on the inbuilt state variable function in COMSOL Multiphysics. It proved to be a useful tool which enabled us to simulate and create changes in electrical quantities which is supposed to represent water tree growth in insulating materials. By changing electrical parameters and conditions for water tree propagation, it is possible to simulate a variety of water trees with different shapes, sizes and propagation rates.

The following sections will present the conclusions that are drawn from the different results. To ensure an easy reading each result with its respective conclusion is presented in its separate section.

5.1.1 Parametric sensitivity analysis

By modeling the water treed region with different values of electrical conductivity and permittivity, it is possible to simulate a variety of water tree patterns as seen in the previous section. The obtained water tree patterns do resemble the experimentally obtained water trees found in the research presented. Since water tree propagation patterns are in a sense unique due to different factors such as the distribution and amount of impurities, two identical test setups may result in different water tree patterns. These various water tree patterns are also realized in the simulations presented since the statistical distribution of impurities may vary depending on how the statistical distribution function is defined.

When comparing the increase in capacitance of this numerical model to other experimental work and numerical work, the increase in capacitance is between the interval for numerical work and measurements conducted on experimental water trees and electrical trees. The laboratory setup, material of the test specimen, and modeling of the damaged region do influence how the water tree propagates as well as what within what range measurements should be taken. In order to confirm how to model water trees using this model, more updated experimental work is needed with accurate measurement methods.

5.1.2 Air layer

From the simulation result it confirms that the presence of an air layer counteracts the propagation of the water tree. It is seen that the water tree propagates at the interface between the two mediums instead of at the tip of the needle, as described in the theory. This concludes that when conducting the water electrode method for water tree experiment, an extra attention should be give to avoid air layers at the tip of water electrode which can influence the water tree propagation.

5.1.3 Effects of material inhomogeneities

The philosophy of the importance of modeling material inhomogeneities still stands. However, this thesis did not arrive at the sought-after results. Instead of a randomly propagating water tree, "bow-tie trees" are introduced in the insulation. These "bow-tie" trees do not exactly follow the physics of real bow-tie trees. They are initiated in the weakened localized bulk of the insulation but they are not limited by any type of impurity stored locally. Since the water tree propagation is exclusively dependent on the electric field, nothing is stopping these bow-tie trees from growing indefinitely. Introducing material imperfections also has an impact on how the capacitance of the system changes when water trees grow in the insulation. Specific statistical functions for each material parameter could provide a more exact solution on how water trees propagate and affect surrounding material.

6
Future work

This section gives a few ideas based on the project group's observations of what could be improved or implemented in future works.

Experimental data
This model is based on the laboratory setup according to the international standard for vented water tree growth but there were no previous publications to be found of work which follow this model and procedure exactly. It would be beneficial for the project if experimental water trees were grown according to the same model in order to compare data. This would enable this project group to adapt and calibrate this model to accurately resemble a real test setup.

Multi-physics coupling
The literature study in this report suggests that several processes are contributing to the development of water trees. It would be interesting to see a multiphysics coupling where mechanical, chemical, and thermo-dynamical phenomena are introduced. This would require an in-depth study as to what phenomenon is more dominating in order to set conditions to water tree propagation. This would include extensive modeling of materials, geometrical setup, and even operational conditions in order to represent the most important reactions taking place during water tree propagation.

Study
This model is based on a series of stationary solutions where each new step is solved with the previous solution as an initial condition. Modeling in the time domain would perhaps yield different results than the ones presented in this report.

Material properties
The solution of modeling inhomogeneous material properties did not achieve the expected result. Instead of a randomly propagating water tree in three dimensions, bow-tie trees are introduced due to weakened insulating properties which cause a localized electric field enhancement. It would be interesting to see if it is possible to accurately model a material with inhomogeneous material properties. This could affect the propagation behavior which has a significant effect on the volume of the water tree which in turns affects the increase in capacitance.

7
Ethics and sustainability

Wind power is mentioned as one of the most credible sources for increasing renewable energy production, especially off-shore wind farms. This report focuses on the water tree phenomena that may develop in the insulation of the subsea cables, but it is still an important part of the wind power farms. The wind farm itself comes with a few uncertainties when placed off-shore. Studies have shown that there are still unknown effects as to what ecological impact these have on marine life, but some studies have shown that all these impacts are not necessarily bad [25].

Usage of subsea cables can be traced back to the mid-19th century, but with the desire to place the wind farms off-shore it has also shed some light on the use of subsea cables. The obvious impact of placing cables at the bottom of the sea is the physical environmental change. Installation, maintenance, and decommissioning can impact the habitats of sea life. There is also the risk of entanglement. Even though these factors impact the environment they are considered minor or short-term. However, the impact of the operation is still unclear. While in operation the cables produce heat, electromagnetic fields, pollution, and reef/reserve effects. There is still a knowledge gap in how these factors affect its surroundings, especially regarding the electromagnetic field and its long-term effects [26].

Although the report itself does not contribute to the knowledge gap described, we hope it can contribute to the understanding of water treeing and how they propagate. By understanding it one can mitigate the risk of degradation thereby increasing the cable's life span, and decreasing the need for maintenance, which in turn decreases the number of physical interventions to the sea floor thereby mitigating the environmental impact.

References

[1] C. N. Sanniyati, Y. Z. Arief, Z. Adzis, N. A. Muhamad, M. H. Ahmad, M. A. B. Sidik, and K. Lau, "Water tree in polymeric cables: a review," *Malaysian Journal of Fundamental and Applied Sciences*, vol. 12, no. 1, pp. 12–21, 2016.

[2] "Standard Test Method for Relative Resistance to Vented Water-Tree Growth in Solid Dielectric Insulating Materials — astm.org," https://www.astm.org/d6097-16.html, [Accessed 11-03-2024].

[3] C. Kim, J. Jang, X. Huang, P. Jiang, and H. Kim, "Finite element analysis of electric field distribution in water treed xlpe cable insulation (1): The influence of geometrical configuration of water electrode for accelerated water treeing test," *Polymer testing*, vol. 26, no. 4, pp. 482–488, 2007.

[4] I. C. U. Ansys GRANTA EduPack software, ANSYS, "Ansys Granta: Materials Information Management — ansys.com," https://www.ansys.com/materials, 2024, [Accessed 25-04-2024].

[5] H. Ritchie, P. Rosado, and M. Roser, "Energy production and consumption," *Our World in Data*, 2020, https://ourworldindata.org/energy-production-consumption.

[6] H. Díaz and C. G. Soares, "Review of the current status, technology and future trends of offshore wind farms," *Ocean Engineering*, vol. 209, p. 107381, 2020.

[7] E. Gulski, G. Anders, R. Jongen, J. Parciak, J. Siemiński, E. Piesowicz, S. Paszkiewicz, and I. Irska, "Discussion of electrical and thermal aspects of offshore wind farms' power cables reliability," *Renewable and Sustainable Energy Reviews*, vol. 151, p. 111580, 2021.

[8] R. Ross, "Inception and propagation mechanisms of water treeing," *IEEE Transactions on Dielectrics and Electrical Insulation*, vol. 5, no. 5, pp. 660–680, 1998.

[9] M. M. Salleh, M. H. I. Saad, Y. Z. Arief, and N. A. Muhamad, "Water tree simulation on underground polymeric cable using finite element method," *Journal of Telecommunication, Electronic and Computer Engineering (JTEC)*, vol. 10, no. 1-12, pp. 107–112, 2018.

[10] J.-P. Crine, "Electrical, chemical and mechanical processes in water treeing," *IEEE Transactions on Dielectrics and Electrical Insulation*, vol. 5, no. 5, pp. 681–694, 1998.

[11] K. Li, K. Zhou, and G. Zhu, "Toward understanding the relationship between the microstructure and propagation behavior of water trees," *IEEE Transactions on Dielectrics and Electrical Insulation*, vol. 26, no. 4, pp. 1116–1124, 2019.

[12] I. Radu, M. Acedo, P. Notingher, F. Frutos, and J. Filippini, "The danger of water trees in polymer insulated power cables evaluated from calculations of electric field in the presence of water trees of different shapes and permittivity distributions," *Journal of Electrostatics*, vol. 40, pp. 343–348, 1997.

[13] J.-P. Crine and J. Jow, "Influence of frequency on water tree growth in various test cells," *IEEE transactions on dielectrics and electrical insulation*, vol. 8, no. 6, pp. 1082–1087, 2001.

[14] S. Grimnes and Ørjan G Martinsen, "Chapter 7 - electrodes," in *Bioimpedance and Bioelectricity Basics (Third Edition)*, third edition ed., S. Grimnes and Ørjan G Martinsen, Eds. Oxford: Academic Press, 2015, pp. 179–254. [Online]. Available: https://www.sciencedirect.com/science/article/pii/B9780124114708000076

[15] I. Radu, M. Acedo, J. Filippini, P. Notingher, and F. Ftutos, "The effect of water treeing on the electric field distribution of xlpe. consequences for the dielectric strength," *IEEE Transactions on Dielectrics and Electrical Insulation*, vol. 7, no. 6, pp. 860–868, 2000.

[16] D. J. Nilsson, S. M. Gubanski, and Y. V. Serdyuk, "Electrical detection of degradation in specimens of hvdc cable insulation," *Energies*, vol. 13, no. 15, p. 3963, 2020.

[17] Y. Yao, T. Han, Q. Li, Y. Huang, and Z. Zheng, "Effect of water tree on broadband impedance spectrum of 10 kv cable," in *2022 IEEE 4th International Conference on Dielectrics (ICD)*. IEEE, 2022, pp. 601–604.

[18] P. Selvamany and G. S. Varadarajan, "An investigation and locating water tree degradation in power cable insulation based on pulse voltage," in *2021 IEEE 5th International Conference on Condition Assessment Techniques in Electrical Systems (CATCON)*. IEEE, 2021, pp. 032–037.

[19] K. Zhou, W. Zhao, and X. Tao, "Toward understanding the relationship between insulation recovery and micro structure in water tree degraded xlpe cables," *IEEE Transactions on Dielectrics and Electrical Insulation*, vol. 20, no. 6, pp. 2135–2142, 2013.

[20] A. Küchler, *High Voltage Engineering: Fundamentals-Technology-Applications*. Springer, 2017.

[21] Q. Wang, Y. Deng, M. Yap, Y. Yang, J. Ma, W. K. Chern, J. Li, and Z. Chen, "Electrical tree modelling in dielectric polymers using a phase-field regularized cohesive zone model," *Materials & Design*, vol. 235, p. 112409, 2023.

[22] K. Morris, "What is hysteresis?" *Applied Mechanics Reviews*, vol. 64, no. 5, p. 050801, 2011.

[23] W. Frei, "How to use state variables in comsol multiphysics®," May 2020. [Online]. Available: https://www.comsol.com/blogs/how-to-use-state-variables-in-comsol-multiphysics/

[24] B. AG, "Borlink™ LS4201R - Borealis — borealisgroup.com," https://www.borealisgroup.com/products/product-catalogue/borlink-ls4201r-1, 2017, [Accessed 03-04-2024].

[25] M. I. G. J. e. a. Galparsoro, I., "Reviewing the ecological impacts of offshore wind farms," https://doi.org/10.1038/s44183-022-00003-5, 2022, [Accessed 25-04-2024].

[26] B. Taormina, J. Bald, A. Want, G. Thouzeau, M. Lejart, N. Desroy, and A. Carlier, "A review of potential impacts of submarine power cables on the marine environment: Knowledge gaps, recommendations and future directions," *Renewable and Sustainable Energy Reviews*, vol. 96, pp. 380–391, 2018.

DEPARTMENT OF ELECTRICAL ENGINEERING
CHALMERS UNIVERSITY OF TECHNOLOGY
Gothenburg, Sweden
www.chalmers.se

CHALMERS
UNIVERSITY OF TECHNOLOGY